Electronic Supplementary Material (ESI) for Molecular Systems Design & Engineering.

Supplementary Information

Surface functionalization of SiC/SiOx nanowires with a fluorinated tetraphenyl-porphyrin: a hybrid nanosystem for X-ray induced singlet oxygen generation

R. Tatti, M. Timpel, M. V. Nardi, F. Fabbri, F. Rossi, L. Pasquardini, A. Chiasera, L. *Aversa, K. Koshmak, A. Giglia, L. Pasquali, T. Rimoldi, L. Cristofolini, G. Attolini, S. Varas, S. Iannotta, R. Verucchi, and G. Salviati*

✓ Detailed Cathodoluminescence (CL) spectra

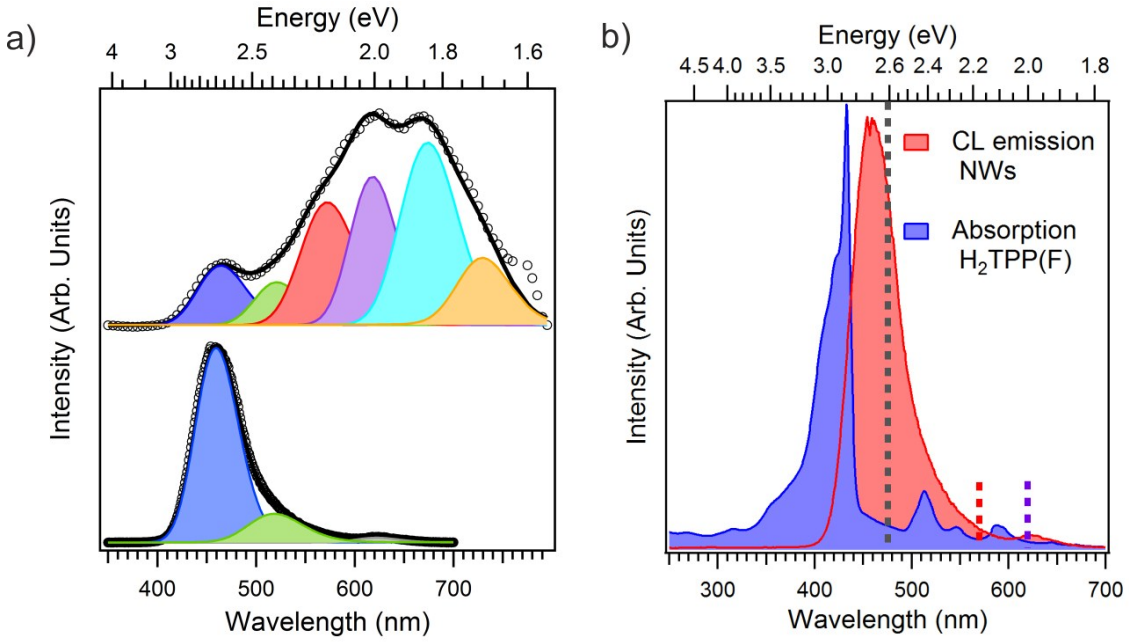

Figure S1. (a) Gaussian deconvolution of the cathodoluminescence (CL) spectra of bare (lower panel) and functionalized NWs (upper panel), to identify the contribution of emission sub-bands. The signal at high wavelength has not been taken into account for the fitting procedure, since it can be attributed to an artefact caused by the cut-off of the detector. (b) CL emission spectrum of bare NWs (red), overlapped with room temperature absorption spectrum of the fluorinated tetraphenyl-porphyrin $H_2TPP(F)$ bulk material (blue). The grey dashed line indicates the excitation wavelength (λ = 458 nm) used for photoluminescence (PL) analysis in the present study (see Fig. 3). The red (violet) dashed line corresponds to the position of the red (violet) component of the CL spectrum in a).

While the bare 3C-SiC/SiO_x core/shell NWs show a CL emission centered in the blue-green region (see Fig. S1a, lower panel), the emission of the hybrid nanosystem (see Fig. S1a, upper panel) is clearly shifted towards the yellow-red spectral region. A Gaussian deconvolution of the spectra highlights that the bare NWs (Fig. S1a, lower panel) have three main emission bands: the blue component, peaked at 2.7 eV, and the yellow one, centred at 1.99 eV, are ascribed to SiO_x related intra-gap states,[1] while the green band is ascribed to near-band-edge (NBE) transitions of the crystalline SiC NW core.[2] After functionalization with H_2TPP(F) (Fig. S1a, upper panel), the NW-related components are still present, but the emission at 2.7 eV is strongly quenched. The cyan and orange components centred at 1.84 eV (*i.e.*, λ = 675 nm) and 1.70 eV (*i.e.*, λ = 730 nm), respectively, are the fingerprint of the functionalization with H_2TPP(F). The energy positions are in agreement with the fluorescence of the H_2TPP(F) bulk material, and can be likely identified as its $Q_x(0,0)$ and $Q_x(0,1)$ transitions. The additional red and violet components at 2.18 eV (*i.e.*, λ = 570 nm) and 2.00 eV (*i.e.*, λ = 620 nm) are most likely emissions stemming from interface levels of the hybrid nanosystem. These peaks are blue-shifted with respect to the fluorescence of the bare H_2TPP(F), and lie in minimum regions of the molecule's absorption spectrum, see red and blue line in Fig. S1b (*i.e.*, no significant re-absorption by the molecule takes place).

✓ **Water contact angles on planar SiO_2 substrate**

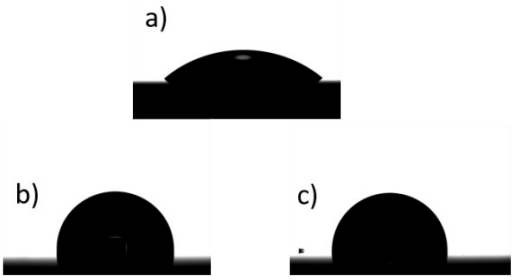

Substrate / Molecule	Thickness	Angle Left / Right
SiO2	-	40.1 / 38.8
SiO2 / H2TPP(F)	Multilayer	98.0 / 97.2
SiO2 / H2TPP(F)	Monolayer*	93.1 / 92.2

Figure S2. Room temperature water contact angles of (a) planar SiO_2 substrate, (b) multilayer of $H_2TPP(F)$, and (c) corresponding monolayer (*after sonication of the multilayer), respectively.

✓ **Orientation of $H_2TPP(F)$ on planar SiO_2 substrate**

XAS measurements have been performed to gain information about the (average) orientation of $H_2TPP(F)$ on the SiO_x surface and to better understand the chemical interaction occurring at the interface between molecule and NWs. As model surface we have used a planar SiO_2 native oxide substrate with a surface roughness of ~5Å.

The XAS experiment on a monolayer of $H_2TPP(F)$ deposited on a planar SiO_2 substrate has been performed at the BEAR end station (BL8.1L), at the left exit of the 8.1 bending magnet of the ELETTRA synchrotron facility in Trieste (Italy).[3,4] All XAS spectra have been collected in total

electron yield (TEY) mode (*i.e.*, drain current mode) at the N K-edge, and have been normalized to the incident photon flux and to the clean substrate signal. The spectral energy has been calibrated by referring to N_2 N 1s−π* transitions. The incidence angle of the light with respect to the sample surface plane has been kept fixed at 10°, and the sample has been rotated around the beam axis to change the polarization from *s* to *p*. This leads to an effective rotation of the electric field plane at the surface while keeping the excitation volume constant. In order to keep both the illuminated area (*i.e.*, the excited volume) and the incidence angle constant, we have changed the direction of the electric field vector $\vec{E}$ from perpendicular to parallel respect to the scattering plane. This has been achieved by rotating the chamber angle ψ_c with respect to the beam axis from $\psi_c = 0°$ (s-scattering) to $\psi_c = 90°$ (p-scattering).[3,4] The synchrotron beam has been linearly polarized (ellipticity $\varepsilon = |\vec{E}_V|^2/|\vec{E}_H|^2 = 0.1$, where V (H) is the vertical (horizontal) direction and ε = 1 (0) for circularly (linearly) polarized light). In order to correctly process the acquired data, each absorption spectrum, collected at different angles ψ_c, has been normalized to the absorption spectrum acquired under the same experimental conditions and the energy range, on an Au(111) sputtered (*i.e.*, carbon free) sample. The energy scale of each single spectrum has been re-calibrated taking into account the energy fluctuation of characteristic absorption features measured on the refocusing mirror.

The XAS spectra of H_2TPP(F) on SiO_2 have been recorded at a coverage of one monolayer (as estimated *via* quartz microbalance). All spectra have been collected from N K-shell electrons excited to unoccupied molecular orbital (MO) levels. Figure S3a shows the XAS spectra collected at four different take-off angles ψ_c spanning from 0° to 90°. Mainly five principal spectral features are identified and labelled as A–E in Figure S3a. On the basis of our previous theoretically calculated absorption spectra of H_2TPP(F),[5] we ascribe the main peak at ~403 eV (labelled as B in Figure S3a) to

transitions from the N 1s to the –C-N π*-antibonding orbital lying within the main molecular plane (see inset in Figure S3b).

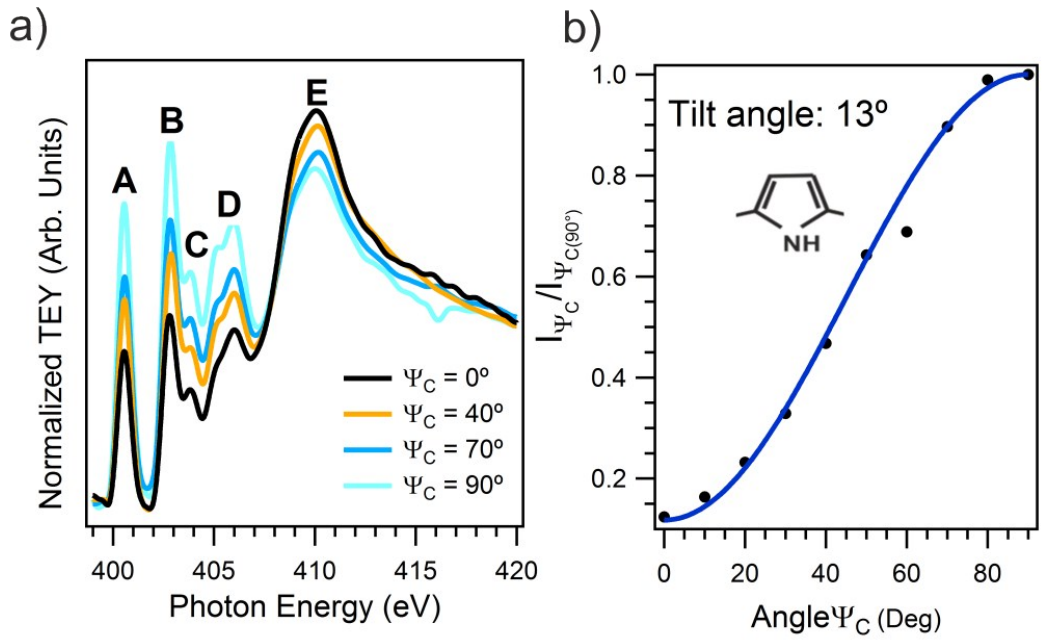

Figure S3. (a) Experimental C K-edge XAS spectra of a monolayer of $H_2TPP(F)$ on a planar SiO_2 substrate. (b) Plot of the relative σ*- and π*-orbital intensities as a function of the angle Ψ_C. The solid curve corresponds to the best fit of the intensity evolution with molecule tilt angle of 13°, referred to the surface normal.

The main peak B exhibits a strong angular dependence, *i.e.*, it is greatly enhanced when the electric field vector is perpendicular to the surface plane (*i.e.*, $\psi_c = 90°$ – p-polarization) but largely attenuated when the electric field is almost parallel to the surface plane (*i.e.*, $\psi_c = 0°$ – s-polarization), suggesting a planar ("flat-lying") orientation of the molecule on the SiO_2 substrate. We have monitored the intensity of feature B collected at 10 different ψ_c angles (see Figure S3b) to better quantify the average orientation of the molecules with respect to the substrate.

Assuming that the molecules at the surface have isotropic azimuthal distribution in the monolayer, the intensity I of a resonance peak corresponding to an excitation into a vector orbital in the used experimental configuration can be described by:[6]

$$\frac{I(\theta)}{I(90°)} = \frac{(\varepsilon^2 cos^2\Psi_c + sin^2\Psi_c)\left(sin^2\theta_M sin^2\theta + cos^2\theta_M cos^2\theta\right) +}{sin^2\theta_M sin^2\theta + cos^2\theta_M cos^2\theta + \varepsilon^2} \quad (1)$$

with θ_M the grazing incidence angle (θ_M = 10°), ψ_c the rotation angle of the analysis chamber at the BEAR beamline with the specific setup used for the measurement, ε the photon ellipticity (ε = 0.1) and θ the tilt angle to be determined. The best fit using equation (1), assuming θ as a free parameter, is shown in Figure S3b and is indicative of an average tilt angle (*i.e.*, main molecular plane with respect to the substrate plane) of ~13°.

- ✓ **Statistical analysis of SOSG fluorescence**

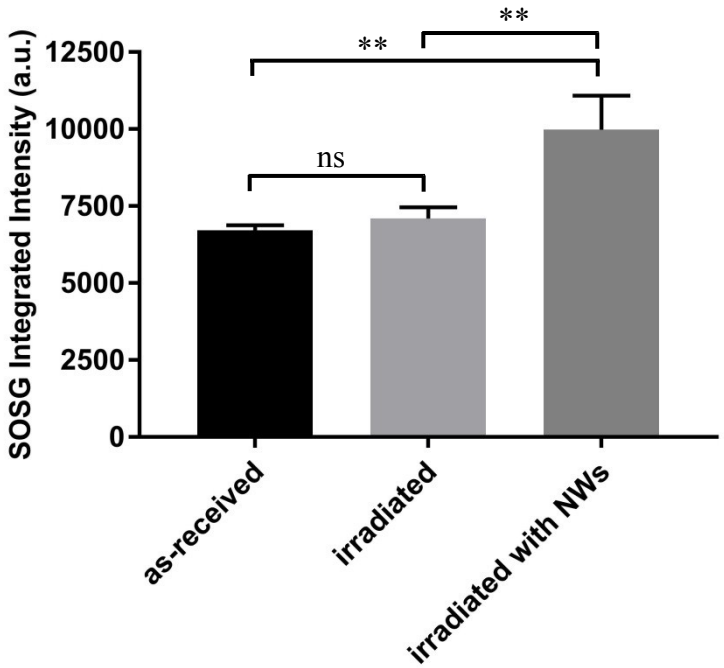

Figure S4. Plot of the SOSG integrated fluorescence intensity of the SOSG marker before X-ray irradiation (as-received), after X-ray irradiation, and after X-ray irradiation in presence of the functionalized NWs. The values correspond to the mean ± standard deviation of 10 repeated experiments.

For statistical analysis of the SOSG fluorescence, the data were analyzed using Prism 7 software (GraphPad, La Jolla, CA, USA), and differences between group means were evaluated by one-way ANOVA with Tukey's multiple comparisons test. The analysis reported in Fig. S4 shows that the fluorescence of the irradiated marker does not significantly differ from the fluorescence of the as-received marker (ns, $p>0.5$). On the contrary, the increase of fluorescence observed when the marker is irradiated with functionalized NWs is statistically significant (**, $0.001 < p < 0.01$), compared to both the as-received and the irradiated-only samples.

1 L. Skuja, *J. Non. Cryst. Solids*, 1998, **239**, 16–48.

2 Y. Goldberg, M. E. Levinshtein and S. L. Rumyantsev, *Properties of Advanced Semiconductor Materials: GaN, AIN, InN, BN, SiC, SiGe*, New York: Wiley, 2001.

3 L. Pasquali, A. DeLuisa and S. Nannarone, *AIP Conf. Proc.*, 2004, **705**, 1142–1145.

4 S. Nannarone, F. Borgatti, A. DeLuisa, B. P. Doyle, G. C. Gazzadi, A. Giglia, P. Finetti, N. Mahne, L. Pasquali, M. Pedio, G. Selvaggi, G. Naletto, M. G. Pelizzo and G. Tondello, *AIP Conf. Proc.*, 2004, **705**, 450–453.

5 M. V. Nardi, R. Verucchi, L. Pasquali, A. Giglia, G. Fronzoni, M. Sambi, G. Mangione and M. Casarin, *Phys. Chem. Chem. Phys.*, 2015, **17**, 2001–2011.

6 L. N. Serkovic Loli, H. Hamoudi, J. E. Gayone, M. L. Martiarena, E. A. Sanchez, O. Grizzi, L. Pasquali, S. Nannarone, B. P. Doyle, C. Dablemont and V. A. Esaulov, *J. Phys. Chem. C*, 2009, **113**, 17866–17875.